5

Prolonged niacin treatment leads to increased adipose tissue PUFA synthesis and an anti-inflammatory lipid and oxylipin plasma profile

Mattijs M. Heemskerk*, Harish K. Dharuri*, Sjoerd A.A. van den Berg, Hulda S. Jónasdóttir, Dick-Paul Kloos, Martin Giera, Ko Willems van Dijk, Vanessa van Harmelen

*Both authors contributed equally

Journal of Lipid Research **2014**, 55(12): 2532-2540

Abstract

Prolonged niacin treatment elicits beneficial effects on the plasma lipid and lipoprotein profile that are associated with a protective cardiovascular disease (CVD) risk profile. Acute niacin treatment inhibits non-esterified fatty acid (NEFA) release from adipocytes and stimulates prostaglandin release from skin Langerhans cells, but the acute effects diminish upon prolonged treatment, while the beneficial effects remain. To gain insight in the prolonged effects of niacin on lipid metabolism in adipocytes, we used a mouse model with a human-like lipoprotein metabolism and drug response (female APOE*3-Leiden. CETP mice) treated with and without niacin for 15 weeks. The gene expression profile of gonadal white adipose tissue (gWAT) from niacin treated mice showed an up-regulation of the "biosynthesis of unsaturated fatty acid (PUFA)" pathway, which was corroborated by qPCR and analysis of the FA ratios in gWAT. Also, adipocytes from niacin treated mice secreted more of the PUFA docosahexaenoic acid (DHA) *ex vivo*. This resulted in an increased DHA/arachidonic acid (AA) ratio in the adipocyte FA secretion profile and in plasma of niacin treated mice. Interestingly, the DHA metabolite 19,20-dihydroxy docosapentaenoic acid (19,20-diHDPA) was increased in plasma of niacin treated mice. Both an increased DHA/AA ratio and increased 19,20-diHDPA are indicative for an anti-inflammatory profile and may indirectly contribute to the atheroprotective lipid and lipoprotein profile associated with prolonged niacin treatment.

Introduction

Niacin (vitamin B3) treatment reduces cardiovascular disease and atherosclerosis development [1]. These beneficial effects are mediated, in part, by lowering circulating levels of LDL-cholesterol, VLDL-TG and lipoprotein(a) [2] as well as by increasing HDL-cholesterol [3]. In addition, prolonged niacin treatment also decreases plasma, adipose tissue and vascular inflammation [4, 5], which might contribute to reducing CVD. The induction of these beneficial effects after prolonged niacin treatment are in striking contrast to the unwanted acute niacin effects.

Acutely, niacin binds to the inhibitory hydroxycarboxylic acid receptor 2 (HCA_2) (previously known as GPR109A). In adipocytes this leads to an inhibition of adipocyte lipolysis followed by an acute reduction of plasma non-esterified fatty acid (NEFA) levels. Lowering NEFA levels causes metabolic stress [6, 7], which increases stress hormone levels [8–12] after niacin treatment. In the skin Langerhans cells and keratinocytes, acute niacin binding to the HCA_2 receptor leads to a release of arachidonic acid (AA) and subsequent cyclooxygenase-mediated oxylipin synthesis (mostly prostaglandins) causing flushing [13] and a decrease in blood pressure [14]. Intriguingly, these acute effects decrease upon prolonged niacin treatment. Adipocyte lipolysis normalizes [15, 16] and flushing diminishes [17].

The fact that certain acute niacin effects decrease over time whereas the beneficial lipid lowering and anti-inflammatory effects remain, suggests differences between the induction of intracellular signaling pathways upon acute and prolonged niacin treatment. In the current study we set out to characterize changes in signaling regulation upon prolonged niacin treatment. We specifically investigated effects of niacin on adipose tissue as adipose tissue has been shown to be the most affected organ at the gene expression level after 7h of niacin treatment [18].

We treated mice with 0.3% niacin mixed through the diet and isolated gonadal white adipose tissue (gWAT) after 15 weeks of intervention. The mice used in this study were female APOE*3-Leiden.CETP mice [19] which-in contrast to wild type mice-have a human like lipoprotein profile and respond similarly to atheroprotective drugs like niacin [20]. A microarray was used to compare gene expression profiles in the adipose tissue. We applied bio-informatic and statistical analyses to the gene expression data and showed that prolonged niacin treatment led to an increase in the pathways unsaturated FA synthesis. To investigate whether PUFA levels and possible derivatives thereof (i.e. oxylipins) were functionally affected we determined the fatty acid (FA) composition in the adipose tissue by gas chromatography mass spectrometry (GC-MS) and measured PUFA and oxylipin profiles in plasma by liquid chromatography tandem mass spectrometry (LC-MS/MS).

Materials and methods

Mouse experiments

Female APOE*3-Leiden.CETP mice were bred at the Leiden University Medical Center. At age 15 ± 1 week, mice were fed a western type diet (Diet T with 0.1 g% cholesterol, which consisted of 16 kcal% protein, 43 kcal% carbohydrate and 41 kcal% fat. AB Diets, Woerden, the Netherlands) with or without niacin (0.3 g%, Sigma Aldrich, St Louis, MO, USA). Supplementary table S2 shows the fatty acid composition of the diet. Body weight was registered weekly. Animals were housed in a controlled environment (21°C, 40-50% humidity) with a daily 12h photoperiod (07h00-19h00). Food and tap water were available ad libitum during the whole experiment. Food intake was determined weekly by weighing the food in the cages at t=0 and at t= 1 days. The difference between these time points was equal to 24h food intake of the mice. The mice in this study are the same as in our previously published study (16). All experiments were performed after a 15 week dietary intervention period. All animals (n=14 per group) were anaesthetized and sacrificed in the fed state between 08h00 and 9h30 by cardiac puncture. Organs and plasma were collected and stored at -80°C. Fresh gonadal white adipose tissue (gWAT) was harvested and kept in PBS with or without niacin. One niacin treated animal did not have sufficient gWAT for the analyses. All animal experiments were performed in accordance with the regulations of Dutch law on animal welfare. The institutional scientific committee and ethics committee for animal procedures from the Leiden University Medical Center, Leiden, The Netherlands approved the protocols.

gWAT gene expression analysis

RNA was isolated from gWAT using the Nucleospin RNA/Protein kit (MACHEREY-NAGEL GmbH & Co. KG, Düren, Germany) after which RNA quality was assessed by NanoDrop (NanoDrop) and 2100 BioAnalyzer (Agilent). All samples had an RNA Integrity Number of >7.5. cRNA was synthesized using the TotalPrep RNA Amplification Kit (Ambion, Illumina). cRNA levels were normalized to 150ng/μL and loaded onto MouseWG-6 v2.0 Expression BeadChips by Service XS (Leiden, The Netherlands). Each BeadChip contains eight arrays. Hybridization and washing were performed according to the Illumina manual. Image analysis and extraction of raw expression data was performed with Illumina GenomeStudio v2011.1 gene expression software with default settings.

Lumi [21] module in the R-based Bioconductor package was used to read in the combined (average) signal intensities per probe. A variance-stabilizing transformation (lumiT) available in the R package was used to stabilize the expression variance based on the bead level expression variance and mean relations. Expression data were normalized using the function lumiN available within the lumi package. We used limma [22] an R-based Bioconductor

package to calculate the level of differential gene expression. In addition to determining significant differentially expressed genes, gene set analysis based on KEGG pathway and Gene Ontology was performed using the Bioconductor package "GlobalTest" [23].

Quantitative PCR

RNA was isolated from gWAT and liver using the Nucleospin RNA/Protein kit (MACHEREY-NAGEL GmbH & Co. KG, Düren, Germany). Subsequently, 1µg of RNA was used for cDNA synthesis by iScript (BioRad, Hercules, CA, USA), which was purified by the Nucleospin Gel and PCR clean-up kit (Machery Nagel). Real-Time PCR was carried out on the IQ5 PCR machine (BioRad) using the Sensimix SYBR Green RT-PCR mix (Quantace, London, UK) and QuantiTect SYBR Green RT-PCR mix (Qiagen, Venlo, the Netherlands). Target mRNA levels were normalized to *Rplp0* & *Ppia* mRNA levels. Primer sequences and PCR conditions can be found in Supplementary table S1.

gWAT, liver and diet fatty acid composition

FA composition analysis of gWAT, liver and diet was carried out as described recently by Kloos *et al.* [24]. Briefly: triplicate samples were weighed of approximately 10 mg diet or organ from niacin treated and control mice. 1 mL of water, 3 mL MeOH and 1 mL 10M NaOH were added, the samples flushed with argon and hydrolyzed for 1 h at 90 °C. After acidification with 2 mL of 6M HCl, 10 µL of an internal standard solution ([$^{2}H_{31}$]palmitic acid and ergosterole 10 µg/mL each) was added. The samples were extracted twice with 3 mL *n*-hexane and the combined organic extracts were dried under a gentle stream of nitrogen. Dried samples were derivatized using 25 µL of *N-tert*.-butyldimethylsilyl-*N*-methyltrifluoroacetamide (Sigma Aldrich, Schnelldorf, Germany) for 10 min at 21 °C, subsequently 25 µL of N,O-bis(trimethylsilyl) trifluoroacetamide containing 1% trimethylchlorosilane (Thermo Scientific, Waltham, MA, USA) and 2.5 µL of pyridine were added and the sample was heated for 15 min to 50 °C. Next, 947.5 µL of n-hexane, containing 10 µg/mL octadecane (C_{18}) as system monitoring component, was added. Samples were analyzed in SIM mode on a Scion TQ GC-MS (Bruker, Bremen, Germany) equipped with a 15 m × 0.25 mm × 0.25 mm BR5MS column (Bruker). The injection volume was 1 µL, the injector was operated in splitless mode at 280 °C and the oven program was as follows: 90 °C kept constant for 0.5 min, then ramped to 180 °C with 30 °C/min then to 250 °C with 10 °C/min then to 266 °C with 2 °C/min and finally to 300 °C with 120 °C/min, kept constant for 2 min. Helium (99.9990%, Air Products, The Netherlands) was used as carrier gas. For data analysis a total area correction was applied and triplicates were averaged.

Gonadal adipocyte PUFA release assay

Fresh gonadal adipose tissue was minced and digested in 0.5 g/L collagenase type I in HEPES buffer (pH 7.4) with 20 g/L of dialyzed bovine serum albumin (BSA, fraction V, Sigma Aldrich) for 1 h at 37°C. The disaggregated WAT was filtered through a nylon mesh with a pore size of 236 µm. For the isolation of mature adipocytes, cells were obtained from the surface of the filtrate and washed several times. Adipocytes (~10,000 cells/mL) were incubated in triplicate in a 96 well plate at 37°C in 200µL per well of DMEM/F12 medium with 2%w/w BSA with or without niacin (10^{-6} M) for 2 hours. The adipocyte conditioned medium (100 µL) was frozen at -20°C until further analysis.

Plasma PUFA and oxylipins measurement

Protein precipitation was performed on adipocyte conditioned medium (80 µL) or plasma (20 µL) by the addition of methanol (233.6 µL for medium and 53.6 µl for plasma) and 6.4 µL of internal standard solution containing ($[^2H_8]$15-HETE, $[^2H_4]PGE_2$, $[^2H_4]LTB_4$ and $[^2H_5]$ DHA, each 50 ng/mL in methanol), which was left to equilibrate for 20 minutes at -20°C. The samples were spun down for 10 min, 16200g at 4°C. Supernatant (240 µL for medium and 30 µL for plasma) was pipetted into a deactivated glass insert (Agilent, CA, USA). Plasma supernatant was diluted in 30 µL of H_2O, while medium supernatant was dried by Speedvac at room temperature. The dried medium sample was dissolved in 60 µL 1:2 methanol/H_2O. For both sample types, 20 µL was injected for LC-MS/MS analysis as described previously [25, 26].

LC-MS/MS analysis is carried out on a QTrap 6500 mass spectrometer (AB Sciex, Nieuwerkerk aan den Ijssel, The Netherlands), coupled to a Dionex Ultimate 3000 LC-system including auto-sampler and column oven (Dionex part of Thermo, Oberschleiβheim, Germany). The employed column was a Kinetex C18 50 × 2.1 mm, 1.7 µm, protected with a C_8 pre-column (Phenomenex, Utrecht, The Netherlands). H_2O (A) and methanol (B) both with 0.01% acetic acid were used. The gradient program started at 40% eluent B and was kept constant for 1 min, then linearly increased to 45% B at 1.1 min, then to 53.5% B at 4 min, to 55% B at 6.5 min, then to 90% B at 12 min and finally to 100% B at 12.1 min, kept constant for 3 min. The flow rate was set to 250.0 µL/min. The MS was operated under the following conditions: the collision gas flow was set to medium, the drying temperature was 400 °C, the needle voltage -4500 V, the curtain gas was 30 psi, ion source gas 1 was 40 psi and the ion source gas 2 was 30 psi (air was used as drying gas and nitrogen as curtain gas). For quantitation, the multiple reaction monitoring (MRM) transitions and collision energies (CE) given in supplementary table S5 were used combined with calibration lines. All substances used as standards were from Cayman Chemicals (Ann Arbor, MI, USA) if not stated otherwise, except RvE1, RvE2 18S-RvE3 and 18R-RvE3 (gifts from Dr. Makoto Arita, Tokyo, Japan). Metabolite identification in plasma was verified by MS/MS spectral comparison with standards, of which leukotriene

E_4, thromboxane B_2 and 19,20-diHDPA are included in the supplements (Supplementary figure S4 until S6).

Statistics

Mean values and standard deviations are reported in all figures. The gene expression data were statistically analyzed by using the multiple test correction method of Benjamin-Hochberg for control of false discovery rate (FDR) for both differentially expressed individual genes and for KEGG pathways. An adjusted p-value < 0.05 was considered significant. Calculations for the lipid measurements were performed in Prism version 6 (GraphPad Software, La Jolla, USA). Multiple T-tests were performed and a 5% FDR value was applied. An F-test was applied to test whether linear regression lines were significantly non-zero. The levels of significance were set at $p < 0.05$.

Results

gWAT gene expression analysis

Female APOE3.Leiden.CETP mice (n=14 per group) were fed a Western type diet (containing 0.1% cholesterol) with and without niacin for 15 weeks. As previously published [16], niacin treatment did not lead to differences in body weight nor gonadal white adipose tissue weight in these mice. However, plasma lipids, i.e. total cholesterol, triglycerides and phospholipids were all decreased [16]. Gene expression analysis generated 24 differentially expressed genes due to niacin treatment after multiple test correction (adjusted $p<0.05$, see Table 1). The global test was applied to identify KEGG pathways affected by niacin treatment. Table 2 depicts the top 5 pathways identified by global test, however only "biosynthesis of unsaturated fatty acids" remained significant after correction for false discovery rate ($q<0.05$). The differentially expressed genes from Table 1 were clustered and highlighted according to KEGG pathways. The top-hits from the "biosynthesis of unsaturated fatty acids" (*Elovl6*, *Tecr* and *Elovl5*) were all specifically involved in FA elongation, not FA desaturation, and were all up-regulated. Quantitative PCR measurements of *Elovl6* and *Elovl5* in gWAT confirmed up-regulation of mRNA levels of these enzymes after niacin treatment (Fig. 1). The rate-limiting desaturase enzyme of PUFA synthesis encoded by *Fads2* (Fatty acid desaturase 2) showed a trend towards increased expression after niacin.

Table 1: Differentially expressed gene hits from microarray analysis of gWAT after niacin treatment. P-value after multiple testing correction. The fold change was calculated as log_2((Niacin/Control). The gene symbols highlighted in black are part of the KEGG pathway "Biosynthesis of unsaturated fatty acids".

Gene symbol	Gene ID	Gene name	Adj. p-value	Log(fold change)
Pdzk1ip1	67182	PDZK1 interacting protein 1	0.002	1.190
Orm2	18406	Orosomucoid 2	0.002	0.857
Orm1	18405	Orosomucoid 1	0.003	0.550
Elovl6	170439	Elongation of long chain fatty acids 6	0.004	1.371
Lctl	235435	Lactase-like	0.004	1.107
Rdh11	17252	Retinol dehydrogenase 11	0.007	0.887
Nudt7	67528	Nudix (nucleoside diphosphate linked moiety X)-type motif 7	0.012	0.537
Acat2	110460	Acetyl-Coenzyme A acetyltransferase 2	0.013	0.695
Mup3	17842	Major urinary protein 3	0.013	1.047
1500017E21Rik	668215	RIKEN cDNA 1500017E21 gene	0.013	0.612
Clstn3	232370	Calsyntenin 3	0.013	0.607
Apoc1	11812	Apolipoprotein C-I	0.013	0.523
Comt	12846	Catechol-O-methyltransferase	0.014	0.536
Zfp385b	241494	Zinc finger protein 385B	0.014	-0.436
Tecr	106529	Trans-2,3-enoyl-CoA reductase	0.029	0.498
G6pdx	14381	Glucose-6-phosphate dehydrogenase X-linked	0.029	0.454
Elovl5	68801	Elongation of long chain fatty acids 5	0.033	0.405
Pkm2	18746	Pyruvate kinase, muscle	0.034	0.521
D430019H16Rik	268595	RIKEN cDNA D430019H16 gene	0.034	-0.505
Aacs	78894	Acetoacetyl-CoA synthetase	0.035	0.524
Lpcat3	14792	Lysophosphatidylcholine acyltransferase 3	0.035	0.504
Kcnj15	16516	Potassium inwardly-rectifying channel, subfamily J, member 15	0.035	0.450
Cyp51	13121	Cytochrome P450, family 51	0.039	0.747
Aard	239435	Alanine and arginine rich domain containing protein	0.039	-0.547
Fasn	14104	Fatty acid synthase	0.126	0.487
Acly	104112	ATP citrate lyase	0.139	0.691

Table 2: Pathways regulated on gene expression level by niacin in the gWAT according to global test. FDR: false discovery rate.

KEGG ID	KEGG pathway name	p-value	FDR q-value
map01040	Biosynthesis of unsaturated fatty acids	1.81E-05	0.00381
map00310	Lysine degradation	7.97E-04	0.16654
map00900	Terpenoid backbone biosynthesis	1.02E-03	0.21273
map00620	Pyruvate metabolism	1.09E-03	0.22603
map00100	Steroid biosynthesis	1.32E-03	0.27205

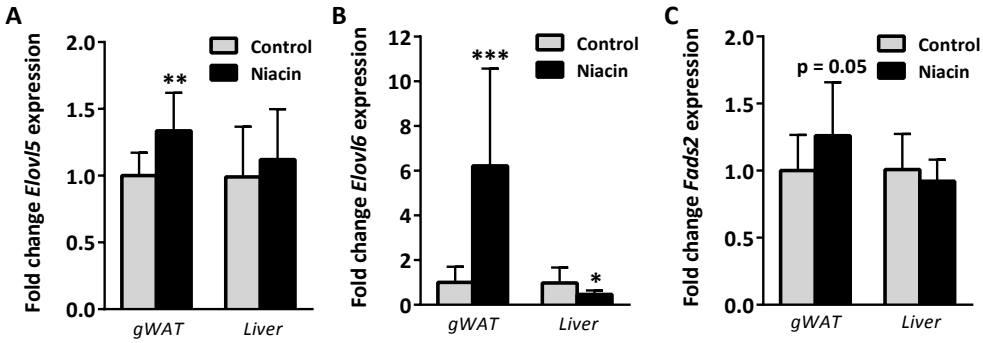

*Figure 1: Gene expression by qPCR of gWAT and liver tissue isolated from unfasted control and niacin treated mice. A) Elovl5, B) Elovl6 and C) Fads2 mRNA levels expressed as fold change from control. *p<0.05, **p<0.01, ***p<0.001 compared to control.*

gWAT fatty acid composition and adipocyte PUFA secretion

To investigate whether the increased mRNA levels of genes in the "biosynthesis of unsaturated fatty acids" translated to adipose tissue FA metabolism changes, we examined the FA composition of the gWAT by GC-MS. In the adipose tissue the fractions of the substrates for PUFA synthesis, the essential fatty acids α-linolenic acid (ALA, n-3) and linoleic acid (LA, n-6), were decreased after niacin treatment while their down-stream products were not fractionally different (Supplementary figure S1 and table S2). As the only source of essential FAs was the diet, of which the consumption was equal (data not shown), an increased enzymatic processing of essential FAs towards down-stream elongated and desaturated PUFAs would be plausible. To examine enzymatic processing, we investigated the substrate/product ratios for the enzymes in the PUFA synthesis pathway. We exclusively found differential elongase ratios and no desaturase ratios between control and niacin treatment (data not shown). Furthermore, the differential ratios that were decreased were the C18 to C20 elongation ratios, while the C20 to C22 ratios were increased indicating a possible increase in the metabolism and processing of essential FAs towards down-stream PUFAs in gWAT from niacin treated mice (Table 3). Given that niacin did no elevate the fractional content of the down-stream

PUFAs of the essential FAs, we studied whether niacin treatment increased PUFA secretion from freshly isolated adipocytes.

Although the fraction of medium chain fatty acids (MCFA, C10:0 / C12:0 / C14:0) was also increased in gWAT after niacin, adipocyte release of these MCFA was not different (Supplemental figure S 7). Of the PUFAs, both ALA and LA were secreted in equal amounts for control and niacin treated adipocytes (Figure 2A). Interestingly, down-stream metabolic products of the essential n-3 fatty acid ALA, namely EPA (non-significant after FRD correction) and DHA, were secreted to a greater extent after niacin treatment.

Table 3: Gene expression level of significant genes in the "Biosynthesis of unsaturated fatty acids" pathway and the associated enzymatic substrate/product ratio of FAs. The fold changes were calculated as log_2(niacin / control).

Gene name	Symbol	Adj. p-value	Fold change	Ratio	p-value	Fold change
Trans-2,3-enoyl-CoA reductase	*Tecr*	0.029	0.498(↑)	General fatty acid elongation		
Elongation of long chain fatty acids 6	*Elovl6*	0.004	1.371(↑)	C16:0 / C18:0	0.416	-0.152(↓)
				C16:1n-9 / C18:1n-9	0.019	-0.370(↓)
Elongation of long chain fatty acids 5	*Elovl5*	0.033	0.405(↑)	C18:3n-3 / C20:3n-3	0.007	-0.619(↓)
				C18:4n-3 / C20:4n-3	Sub & prod not measured	
				C18:2n-6 / C20:2n-6	0.028	-0.540(↓)
				C18:3n-6 / C20:3n-6	0.049	-0.390(↓)
Elongation of long chain fatty acids 5/2	*Elovl5/ Elovl2*			C20:5n-3 / C22:5n-3	0.155	0.529(↑)
				C20:4n-6 / C22:4n-6	0.032	0.387(↑)

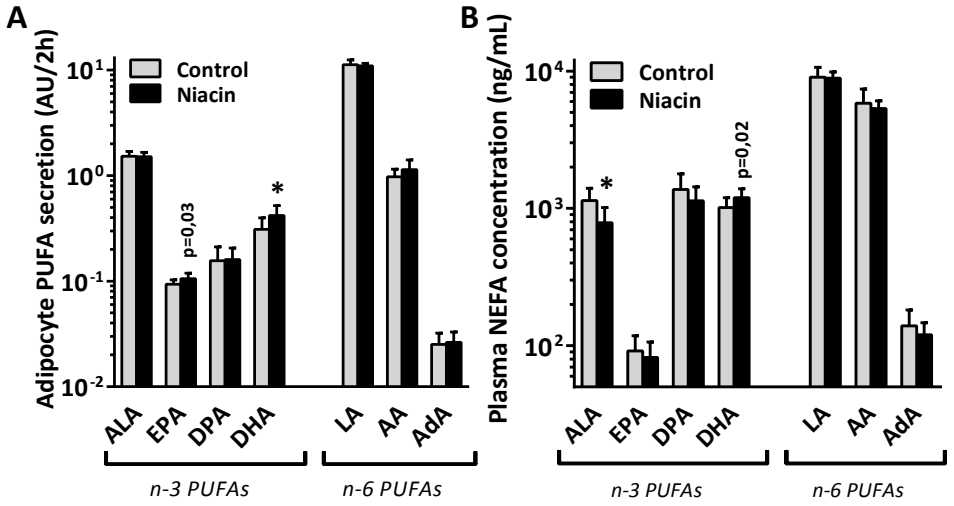

*Figure 2: A) PUFA release from ex vivo isolated adipocytes from control and niacin treated mice incubated for two hours in DMEM/F12 medium. B) PUFA concentration in unfasted plasma of control and niacin treated mice. Mean±SD, n=14 for Control/n=13 for Niacin. *p<0.05 compared to control gWAT after FDR correction. P-values listed were before FDR correction.*

Liver PUFA biosynthesis gene expression and fatty acid composition

As adipose tissue and the liver are the main sites of NEFA processing, we also examined the effects of prolonged niacin on the liver. We found by using qPCR that *Elovl5* and *Fads2* expression were unaffected by niacin treatment, while *Elovl6* expression was down-regulated (Figure 1). Liver fatty acid composition did not differ between control and niacin treated mice (supplementary figure S2 and table S3), neither did the substrate/product ratios relevant for PUFA biosynthesis (Data not shown). Although the PUFA fractions of the livers from niacin treated mice went in the inverse direction as seen in gWAT, this effect was non-significant.

Plasma PUFAs and oxylipins

In addition to measuring PUFA levels in adipocyte medium *ex vivo* we also examined PUFA levels in plasma by LC-MS/MS. Niacin reduced circulating levels of ALA and tended to increase the levels of its down-stream product DHA (Figure 2B and supplementary table S4, DHA was NS after FDR correction). EPA levels were not affected by niacin. We next examined the ratio of DHA over AA as a surrogate marker for PUFA associated cardiovascular risk [27–29] and found that the ratio was shifted towards DHA, both in adipocyte medium and in plasma (Figure 3A). PUFA derived oxylipin signaling molecules were also measured in the plasma (Figure 3B and supplementary table S4). Arachidonic acid metabolite prostaglandin

D_2 was not affected by niacin treatment, whereas thromboxane B_2 levels increased (NS after FDR correction). AA metabolite leukotriene E_4 decreased after niacin treatment (NS after FDR correction), whereas 12-hydroxy eicosatetraenoic acid (12-HETE) levels remained unchanged. The n-3 PUFA derived diol metabolite 19,20-dihydroxy docosapentaenoic acid (19,20-diHDPA) produced by cytochrome P450 was significantly increased. Due to the increase in DHA levels we investigated the presence of DHA derived resolvins [30], which could however not be detected by our approach.

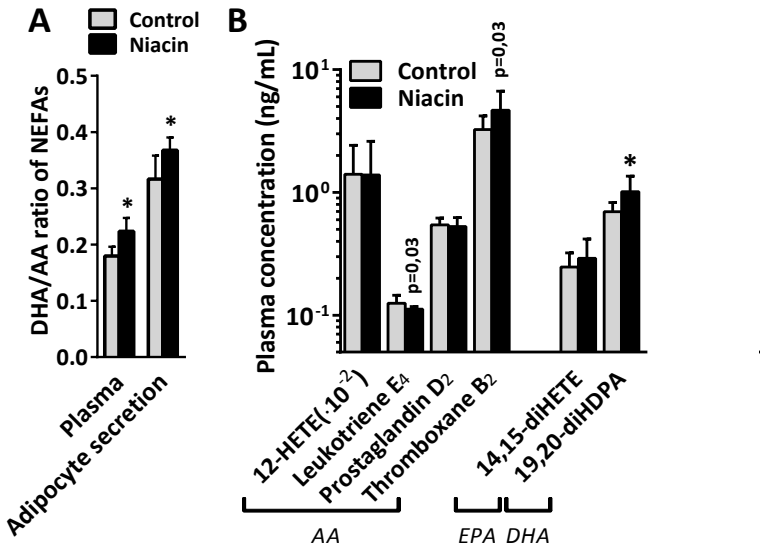

*Figure 3: A) Docosahexaenoic acid over arachidonic acid ratio in adipocyte secreted medium and in plasma. B) Oxylipin concentration in plasma of control and niacin treated mice. Mean±SD, n=14 per group. *p<0.05 compared to control gWAT after FDR correction. P-values listed were before FDR correction.*

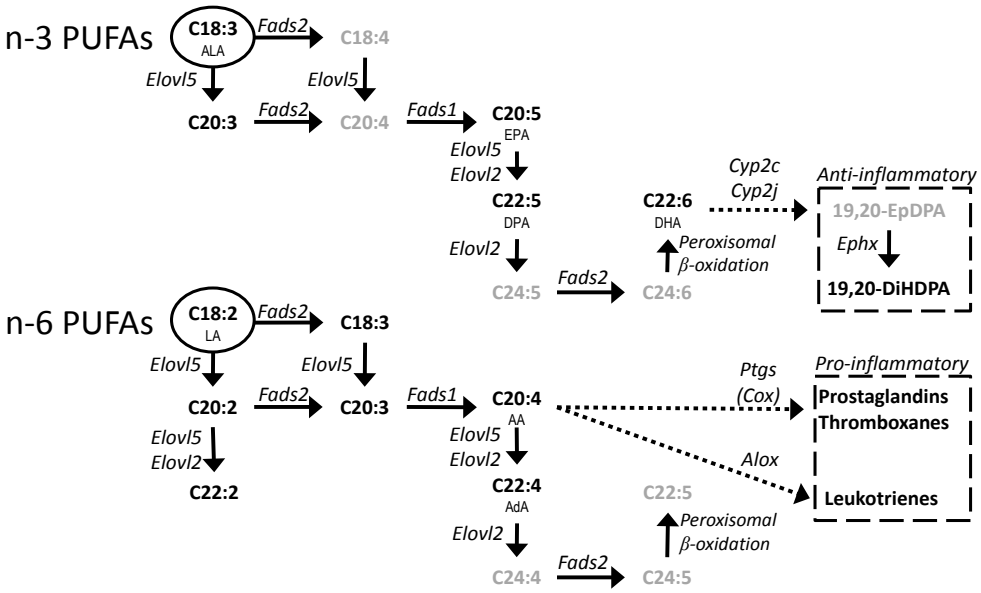

Figure 4: Schematic overview of the synthesis of poly unsaturated fatty acids and the subsequent conversion to a selection of oxylipins. Genes are in italic, metabolites in bold and essential FAs are encircled. Metabolites in grey were not measured. Based on the review by Guillou et al.[31]

Discussion

The current study demonstrates for the first time that prolonged niacin treatment results in an up-regulation of the n-3 PUFA synthesis pathway in adipose tissue. Gene expression analysis of gWAT showed that our hyperlipidemic mouse model responded to niacin by up-regulating genes involved in the unsaturated FA biosynthesis. Fatty acid composition analysis corroborated the increased PUFA synthesis. A higher degree of n-3 PUFA secretion from prolonged niacin treated adipocytes was seen, which was also reflected in increased n-3 PUFA plasma levels. Markedly, the plasma levels of n-3 PUFA derived oxylipins produced by cytochrome P450 and hydrolyzed by soluble epoxy hydrolases were increased. Oxylipins produced by cytochrome P450 from n-3 PUFAs and the n-3 PUFAs themselves suggest a beneficial vascular health profile, which might contribute to the prolonged niacin-induced atheroprotective effect.

Gene expression analysis of the gonadal white adipose tissue of hyperlipidemic mice treated with niacin for 15 weeks demonstrated an up-regulation of the "biosynthesis of unsaturated fatty acid" pathway, mostly by up-regulation of *Elovl6*, *Tecr* and *Elovl5*. All three genes are involved in FA elongation, not desaturation (as shown in figure 4 and table 3). This discovery was confirmed by qPCR, but also by gWAT FA composition and FA ratio analysis, which all pointed towards PUFA elongation. This increase in PUFA elongation was seen in adipose tissue, but not in liver tissue, where a more inverse trend towards PUFA accumulation could be seen in the fatty acid composition. When examining the PUFA secretion of adipocytes isolated from these mice, we found that specifically end-products of n-3 PUFA biosynthesis were secreted to a higher degree, as seen by DHA (C22:6) and also by EPA (C20:5) secretion. As the genes involved in PUFA biosynthesis are the same for n-3 PUFAs as for n-6 PUFAs, the specificity for increased n-3 PUFA secretion was puzzling. It is conceivable that the PUFA biosynthesis enzymes have a higher affinity for n-3 PUFAs, as was already shown for zebrafish desaturase enzymes [32]. The rat elongase 5 enzyme possesses a higher affinity for n-3 substrates than for n-6 substrates [33], and the mouse equivalent was found to be up-regulated in our study. Selective DHA biosynthesis, unlike AA or EPA, requires partial peroxisomal beta oxidation (Figure 4). Although the microarray did not point towards this pathway, increased peroxisomal beta oxidation after niacin could lead to preferential DHA synthesis. Asides from preferential n-3 PUFA biosynthesis, preferential mobilization from adipose tissue would also explain an increased n-3 PUFA release. A well-documented phenomenon is selective PUFA release from adipocytes [34], exemplified by fasting-induced preferential n-3 PUFA depletion of adipose tissue triglycerides [35]. Our preliminary results also indicate preferential n-3 PUFA release from adipocytes when (fasting-induced) lipolysis is stimulated by 8Br-cAMP (Supplemental figure S8c). Other potential mechanisms for preferential n-3 PUFA release might be phospholipid hydrolysis, as it has been previously shown that cytosolic PLA_2 releases AA and EPA from phospholipids whereas the release of DHA from phospholipids requires calcium-independent PLA_2 [36]. Although 99% of the

fatty acids are located in the triglyceride fraction, the contribution of the 1% fatty acids contained in the phospholipid fraction to n-3 PUFA release cannot be excluded. Additional research is required to investigate the underlying mechanisms for the preferential n-3 PUFA release after prolonged niacin treatment.

Adipocyte lipolysis contributes to the free fatty acid pool in the circulation. In the plasma of the niacin treated animals, we found a tendency for increased levels of the n-3 PUFA DHA in the NEFA pool. Although we do not have direct proof, our data suggest that DHA secretion by adipocytes is the main source of DHA in the plasma. Interestingly we did not find up-regulation of gene expression levels of *Elovl5*,*Elovl6* nor *Fads2*, or any change in fatty acid composition in the livers of the niacin treated mice, indicating that the niacin induced PUFA synthesis is selective for adipose tissue.

The n-3 PUFAs have been reported to confer CVD protective abilities via their conversion to anti-inflammatory oxylipins. For example, DHA can be converted to the oxylipin 19(20)-epoxy docosapentaenoic acid (19(20)-EpDPA) by cytochrome P450 (CYP) as can be seen in figure 4. Likewise, the n-3 PUFA EPA can be converted to 14(15)-epoxy eicosatetraenoic acid (14(15)-EpETE) by CYP. These epoxide metabolites have powerful biological effects on cardiovascular health. This was shown by previous studies where the epoxide metabolism pathway was genetically manipulated [37] or its compounds were pharmacologically elevated [38]. These studies showed the importance of epoxy metabolites in resolving inflammation, preserving vascular tone and general vascular homeostasis. The biologically active 19(20)-EpDPA and 14(15)-EpETE can be hydrolyzed by soluble epoxy hydrolases (encoded by the *Ephx2* gene in mice) to their respective diol metabolites 19,20-diHDPA and 14,15-dihydroxy eicosatetraenoic acid (14,15-diHETE). The levels of both these diol products were increased in plasma of niacin treated animals. The hydrolyzed diol metabolites have a far lower biological effect than their epoxide metabolites, but are more stable and can be detected in plasma by LC-MS/MS. Although we did not directly measure whether the levels of the bioactive epoxy metabolites 19(20)-EpDPA or 14(15)-EpETE were increased after niacin treatment, we found a positive correlation in plasma between the precursor and diol metabolite of 19(20)-EpDPA (DHA and 19,20-diHDPA) in niacin treated mice (Supplementary figure S3). This correlation suggests that the levels of 19(20)-EpDPA must also have increased after niacin treatment.

In general, the anti-inflammatory oxylipins such as epoxy metabolites produced by CYP (high affinity for n-3 PUFAs), are balanced by the pro-inflammatory oxylipins such as those produced by cyclooxygenases (COX) and arachidonate lipoxygenases (ALOX) (both with high affinity for n-6 PUFAs, such as AA) [39]. Prolonged niacin treatment did not dramatically affect AA derived oxylipin levels, although there was a tendency towards decreased levels of leukotriene E_4, a lipoxygenase pathway product stimulating inflammation, and towards increased levels of thromboxane B_2, a cyclooxygenase product stimulating coagulation.

Acute treatment of mouse adipocytes with niacin did not lead to an increased release of DHA or AA, nor a change in the ratio of DHA/AA in the adipocyte conditioned medium

(Supplemental figure S 9). Acute niacin treatment however, is a well-known trigger for AA-derived oxylipin synthesis in the skin. Irritative subcutaneous skin flushing is a common acute side-effect of niacin, induced by cyclooxygenase product prostaglandin D_2 [40] in Langerhans cells and keratinocytes. As mentioned above, we did not see an increase in pro-inflammatory prostaglandins after prolonged niacin treatment. These results are in line with results by Stern *et al.* [17] and suggest tolerance for flushing after prolonged niacin treatment. It is possible that the tolerance for flushing after prolonged niacin is mediated via n-3 PUFAs as suggested by vanHorn *et al.* [41]. Whether there is a role for anti-inflammatory n-3 PUFA derived oxylipins after acute niacin remains unclear. Inceoglu *et al.* [42] have acutely administered niacin to mice being treated with a soluble epoxide hydrolase inhibitor, which resulted in a blunted flushing response compared to wild type mice, while acute prostaglandin D_2 treatment did not blunt flushing. These results support a role for cytochrome P450 epoxide metabolites not only after prolonged niacin treatment, but also acutely in inhibiting the flushing response by niacin. Flushing severity also suggests an important balance between pro- and anti-inflammatory oxylipins, which can be modulated by niacin treatment. Most likely, the n-6 derived oxylipins prevail during acute niacin treatment, while after prolonged niacin treatment the n-3 derived oxylipins prevail.

Plasma DHA/AA ratio has been shown to be a diagnostic marker for PUFA associated cardiovascular health [27–29]. In addition to being metabolized to anti-inflammatory oxylipins, n-3 PUFA confer their CVD protective abilities by direct competition with n-6 PUFAs. Vanhorn *et al.* [41] have described that DHA supplementation increases the DHA/AA ratio in membrane phospholipids of Langerhans cells, thereby diminishing the relative availability of AA for pro-inflammatory prostaglandin synthesis. As a low n-3/n-6 ratio is associated with a risk for cardiovascular disease, increasing the ratio by supplementary n-3 PUFAs has been posed as a treatment target [43]. In our study, we see that the DHA/AA ratio has increased towards the anti-inflammatory DHA side without supplementary n-3 PUFAs. We have seen this increased DHA/AA ratio in both the *ex vivo* adipocyte PUFA secretion profile and in the *in vivo* plasma NEFA profile of niacin treated mice. These effects of niacin on adipose tissue and plasma PUFAs and oxylipins pose a potential contributing mechanism by which niacin treatment reduces cholesterol levels and CVD risk. Although we used mice in this study which are human like with respect to lipoprotein profile it remains to be investigated whether there are changes in the plasma DHA/AA ratio in humans treated with niacin.

In conclusion, prolonged niacin treatment of our hyperlipidemic mouse model with niacin resulted in up-regulation the entire pathway of PUFA biosynthesis in gWAT, increased n-3 PUFA secretion from the adipocytes and an increased plasma level of n-3 PUFAs and their anti-inflammatory oxylipins, which together point towards an atheroprotective plasma profile induced by prolonged niacin treatment.

Acknowledgements

This work was supported by grants from Center of Medical Systems Biology (CMSB), the Netherlands Consortium for Systems Biology (NCSB) established by The Netherlands Genomics Initiative/Netherlands Organization for Scientific Research (NGI/NWO), Leiden University Medical Center. Hulda Jónasdóttir is partially funded by the Stichting Prof. Jan Veltkamp Fonds (LUMC). This study was performed within the framework of the Center for Translational Molecular Medicine (http://www.ctmm.nl); project PREDICCt (grant 01C-104). We thank Dr. Makoto Arita from the department of Health Chemistry Graduate School of Pharmaceutical Sciences, University of Tokyo, Japan, for the kind gift of RvE1, RvE2, 18S-RvE3 and 18R-RvE3 used as standard material in the employed LC-MS/MS platform. The authors declare that there is no duality of interest associated with this manuscript.

References

1 Bruckert E, Labreuche J *et al.* **2010**; Meta-analysis of the effect of nicotinic acid alone or in combination on cardiovascular events and atherosclerosis. *Atherosclerosis* 210:353.

2 Morgan JM, Capuzzi DM *et al.* **2003**; Effects of extended-release niacin on lipoprotein subclass distribution. *American journal of cardiology* 91:1432.

3 Hernandez M, Wright SD *et al.* **2007**; Critical role of cholesterol ester transfer protein in nicotinic acid-mediated HDL elevation in mice. *Biochemical and biophysical research communications* 355:1075.

4 Wanders D, Graff EC *et al.* **2013**; Niacin Increases Adiponectin and Decreases Adipose Tissue Inflammation in High Fat Diet-Fed Mice. *PLoS ONE* 8:e71285.

5 Wu BJ, Chen K *et al.* **2012**; Niacin inhibits vascular inflammation via the induction of heme oxygenase-1. *Circulation* 125:150.

6 Chen X, Iqbal N *et al.* **1999**; The effects of free fatty acids on gluconeogenesis and glycogenolysis in normal subjects. *Journal of clinical investigation* 103:365.

7 Kasalicky J, Konopkova M *et al.* **2001**; 18F-fluorodeoxyglucose accumulation in the heart, brain and skeletal muscle of rats; the influence of time after injection, depressed lipid metabolism and glucose-insulin. *Nuclear medicine review. Central & Eastern Europe* 4:39.

8 Kaushik SV, Plaisance EP *et al.* **2009**; Extended-release niacin decreases serum fetuin-A concentrations in individuals with metabolic syndrome. *Diabetes/metabolism research and reviews* 25:427.

9 O'Neill M, Watt MJ *et al.* **2004**; Effects of reduced free fatty acid availability on hormone-sensitive lipase activity in human skeletal muscle during aerobic exercise. *Journal of applied physiology* 97:1938.

10 Oh YT, Oh K-S *et al.* **2011**; Continuous 24-h Nicotinic Acid Infusion in Rats Causes FFA Rebound and Insulin Resistance by Altering Gene Expression and Basal Lipolysis in Adipose Tissue. *American journal of physiology. Endocrinology and metabolism* 300:1012.

11 Quabbe H-J, Luyckx AS *et al.* **1983**; Growth Hormone, Cortisol, and Glucagon Concentrations during Plasma Free Fatty Acid Depression: Different Effects of Nicotinic Acid and an Adenosine Derivative (BM 11.189). *Journal of clinical endocrinology and metabolism* 57:410.

12 Watt MJ, Holmes AG *et al.* **2004**; Reduced plasma FFA availability increases net triacylglycerol degradation, but not GPAT or HSL activity, in human skeletal muscle. *American journal of physiology. Endocrinology and metabolism* 287:E120.

13 Hanson J, Gille A *et al.* **2010**; Nicotinic acid- and monomethyl fumarate-induced flushing involves GPR109A expressed by keratinocytes and COX-2-dependent prostanoid formation in mice. *Journal of clinical investigation* 120:2910.

14 Gadegbeku CA, Dhandayuthapani A *et al.* **2003**; Hemodynamic effects of nicotinic acid infusion in normotensive and hypertensive subjects. *American journal of hypertension* 16:67.

15 Wang W, Basinger A *et al.* **2000**; Effects of nicotinic acid on fatty acid kinetics, fuel selection, and pathways of glucose production in women. *American journal of physiology. Endocrinology and metabolism* 279:E50.

16 Heemskerk MM, van den Berg SA *et al.* **2014**; Long-term niacin treatment induces insulin resistance and adrenergic responsiveness in adipocytes by adaptive downregulation of phosphodiesterase 3B. *American journal of physiology. Endocrinology and metabolism* 306:E808.

17 Stern RH, Spence JD *et al.* **1991**; Tolerance to nicotinic acid flushing. *Clinical pharmacology and therapeutics* 50:66.

18 Choi S, Yoon H *et al.* **2011**; Widespread effects of nicotinic acid on gene expression in insulin-sensitive tissues: implications for unwanted effects of nicotinic acid treatment. *Metabolism* 60:134.

19 Westerterp M, van der Hoogt CC *et al.* **2006**; Cholesteryl ester transfer protein decreases high-density lipoprotein and severely aggravates atherosclerosis in APOE*3-Leiden mice. *Arteriosclerosis, Thrombosis, and Vascular Biology* 26:2552.

20 Kuhnast S, Louwe MC *et al.* **2013**; Niacin Reduces Atherosclerosis Development in APOE*3Leiden.CETP Mice Mainly by Reducing NonHDL-Cholesterol. *PLoS ONE* 8:e66467.

21 Du P, Kibbe WA *et al.* **2008**; lumi: a pipeline for processing Illumina microarray. *Bioinformatics* 24:1547.

22 Smyth GK. **2004**; Linear models and empirical bayes methods for assessing differential expression in microarray experiments. *Statistical applications in genetics and molecular biology* 3:3.

23 Goeman JJ, van de Geer SA *et al.* **2004**; A global test for groups of genes: testing association with a clinical outcome. *Bioinformatics* 20:93.

24 Kloos DP, Gay E *et al.* **2014**; Comprehensive GC–MS analysis of fatty acids and sterols using sequential one-pot silylation: quantification and isotopologue analysis. *Rapid communnications in mass spectrometry* 28:1507.

25 Giera M, Ioan-Facsinay A *et al.* **2012**; Lipid and lipid mediator profiling of human synovial fluid in rheumatoid arthritis patients by means of LC-MS/MS. *Biochimica et biophysica acta* 1821:1415.

26 Yang R, Chiang N *et al.* **2011**; Metabolomics-lipidomics of eicosanoids and docosanoids generated by phagocytes. *Current protocols in immunology* 14:26.

27 Nozue T, Yamamoto S *et al.* **2014**; Low serum docosahexaenoic acid is associated with progression of coronary atherosclerosis in statin-treated patients with diabetes mellitus: results of the treatment with statin on atheroma regression evaluated by intravascular ultrasound with virtual histology (TRUTH) study. *Cardiovascular diabetology* 13:13.

28 Nishizaki Y, Shimada K *et al.* **2014**; Significance of imbalance in the ratio of serum n-3 to n-6 polyunsaturated fatty acids in patients with acute coronary syndrome. *American journal of cardiology* 113:441.

29 Dohi T, Miyauchi K *et al.* **2011**; Long-term impact of mild chronic kidney disease in patients with acute coronary syndrome undergoing percutaneous coronary interventions. *Nephrology, dialysis, transplantation* 26:2906.

30 Serhan CN, Petasis NA. **2011**; Resolvins and protectins in inflammation resolution. *Chemical reviews* 111:5922.

31 Guillou H, Zadravec D *et al.* **2010**; The key roles of elongases and desaturases in mammalian fatty acid metabolism: Insights from transgenic mice. *Progress in lipid research* 49:186.

32 Hastings N, Agaba M *et al.* **2001**; A vertebrate fatty acid desaturase with Δ5 and Δ6 activities. *Proceedings of the National Academy of Sciences* 98:14304.

33 Gregory MK, Gibson RA *et al.* **2011**; Elongase Reactions as Control Points in Long-Chain Polyunsaturated Fatty Acid Synthesis. *PLoS ONE* 6:e29662.

34 Raclot T. **2003**; Selective mobilization of fatty acids from adipose tissue triacylglycerols. *Progress in lipid research* 42:257.

35 Nieminen P, Mustonen A-M *et al.* **2009**; Fatty Acid Composition and Development of Hepatic Lipidosis During Food Deprivation—Mustelids as a Potential Animal Model for Liver Steatosis. *Experimental biology and medicine* 234:278.

36 Strokin M, Sergeeva M *et al.* **2003**; Docosahexaenoic acid and arachidonic acid release in rat brain astrocytes is mediated by two separate isoforms of phospholipase A2 and is differently regulated by cyclic AMP and Ca2+. *British journal of pharmacology* 139:1014.

37 Imig JD. **2012**; Epoxides and Soluble Epoxide Hydrolase in Cardiovascular Physiology. *Physiological reviews* 92:101.

38 Askari AA, Thomson S *et al.* **2014**; Basal and inducible anti-inflammatory epoxygenase activity in endothelial cells. *Biochemical and biophysical research communications* 446:633.

39 Fischer R, Konkel A *et al.* **2014**; Dietary Omega-3 Fatty Acids Modulate the Eicosanoid Profile in Man Primarily via the CYP-epoxygenase Pathway. *Journal of Lipid Research* 55:1150.

40 Serebruany V, Malinin A *et al.* **2010**; The in vitro effects of niacin on platelet biomarkers in human volunteers. *Thrombosis and haemostasis* 104:311.

41 Vanhorn J, Altenburg JD *et al.* **2012**; Attenuation of niacin-induced prostaglandin D(2) generation by omega-3 fatty acids in THP-1 macrophages and Langerhans dendritic cells. *Journal of inflammation research* 5:37.

42 Inceoglu AB, Clifton HL *et al.* **2012**; Inhibition of soluble epoxide hydrolase limits niacin-induced vasodilation in mice. *Journal of cardiovascular pharmacology* 60:70.

43 Simopoulos AP. **2008**; The Importance of the Omega-6/Omega-3 Fatty Acid Ratio in Cardiovascular Disease and Other Chronic Diseases. *Experimental biology and medicine* 233:674.

Supplemental data

Table S1:

Gene	Forward primer	Reverse primer	Temperature
Rplp0	GGACCCGAGAAGACCTCCTT	GCACATCACTCAGAATTTCAATGG	60
Ppia	ACTGAATGGCTGGATGGCAA	TGTCCACAGTCGGAAATGGT	61
Elovl5	CAGCTTGCTTCTGTTCCCG	TCCATTTTAAAACCTCTCTGCCT	61
Elovl6	GCACTAAGACCGCAAGGCAT	CTACGTGTTCTCTGCGCCTC	61
Fads2	CTGGTGGAACCACCGACATT	TCTTGCCATACTCAAGGGGC	61

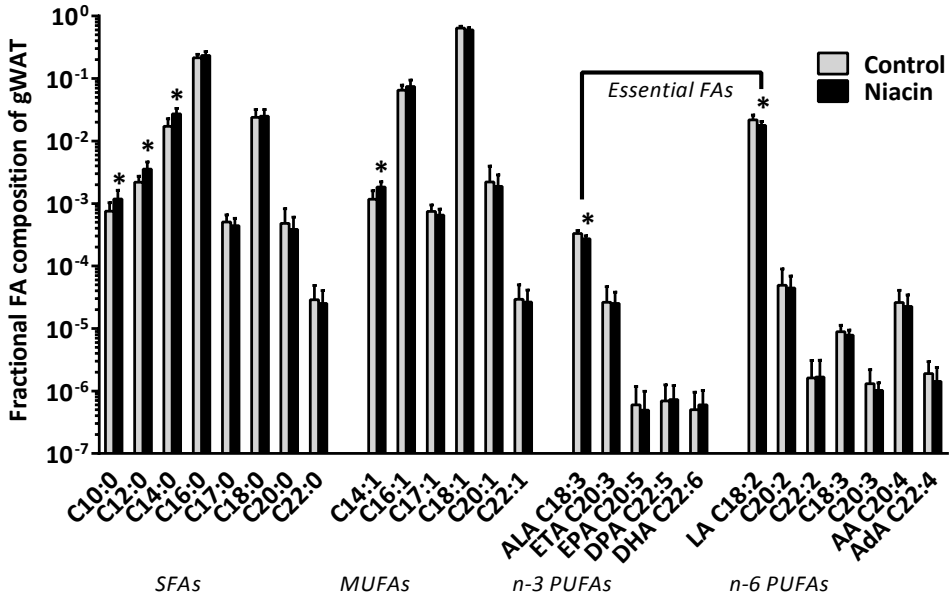

*Figure S1: Adipose tissue fatty acid composition of gWAT from APOE*3-Leiden.CETP mice fed a western type diet with 0.1% cholesterol with and without niacin. Mean±SD, N=14 for Control/N=13 for Niacin, *p<0.05 compared to control gWAT after false discovery rate correction.*

*Table S 2: Adipose tissue fatty acid composition of gWAT from APOE*3-Leiden.CETP mice fed a western type diet with 0.1% cholesterol with and without niacin and fatty acid composition of the western type diet. Fraction of total area corrected sum. Mean±SD, N=14 for Control/N=13 for Niacin/N=3 for diet. (*)Significant finding after false discovery rate correction.*

	Control gWAT		Niacin gWAT		Diet		Control vs Niacin
	Average	SD	Average	SD	Average	SD	P-value
SFA							
C10:0	0,0008	0,0003	0,0012	0,0004	0,0013	0,0009	(*)0,0078
C12:0	0,0022	0,0005	0,0036	0,0011	0,0019	0,0013	(*)0,0005
C14:0	0,0173	0,0054	0,0271	0,0061	0,0059	0,0038	(*)0,0003
C16:0	0,2153	0,0285	0,2339	0,0360	0,4351	0,0571	0,1679
C17:0	0,0005	0,0002	0,0004	0,0001	0,0014	0,0006	0,2804
C18:0	0,0239	0,0081	0,0250	0,0069	0,2162	0,0331	0,7049
C20:0	0,0005	0,0003	0,0004	0,0002	0,0030	0,0009	0,4066
C22:0	2,88E-05	1,99E-05	2,51E-05	1,55E-05	3,00E-04	7,01E-05	0,6070
MUFA							
C14:1	0,0012	0,0004	0,0018	0,0004	0,0003	0,0002	(*)0,0006
C16:1	0,0652	0,0131	0,0745	0,0202	0,0055	0,0035	0,1773
C17:1	0,0007	0,0002	0,0007	0,0002	0,0002	0,0001	0,1951
C18:1	0,6400	0,0459	0,6007	0,0532	0,3036	0,0445	0,0593
C20:1	0,0022	0,0018	0,0019	0,0010	0,0004	0,0002	0,5577
C22:1	2,94E-05	2,05E-05	2,65E-05	1,47E-05	1,62E-05	1,13E-05	0,6729
PUFA n-3							
ALA C18:3	3,32E-04	3,89E-05	2,72E-04	3,37E-05	4,58E-04	9,25E-05	(*)0,0003
ETA C20:3	2,63E-05	2,06E-05	2,51E-05	1,31E-05	2,82E-06	1,61E-06	0,8598
EPA C20:5	6,01E-07	5,83E-07	4,93E-07	4,93E-07	9,89E-07	9,91E-07	0,7985
DPA C22:5	6,95E-07	5,62E-07	7,28E-07	5,00E-07	4,11E-07	3,58E-07	0,8961
DHA C22:6	5,02E-07	4,58E-07	6,00E-07	4,28E-07	2,06E-06	4,75E-07	0,5940
PUFA n-6							
LA C18:2	2,19E-02	4,13E-03	1,78E-02	2,82E-03	2,32E-02	9,00E-03	(*)0,0080
C20:2	4,91E-05	4,09E-05	4,43E-05	2,49E-05	1,15E-05	4,28E-06	0,7206
C22:2	1,62E-06	1,47E-06	1,67E-06	1,45E-06	7,95E-06	1,70E-06	0,9370
C18:3	8,86E-06	2,45E-06	7,84E-06	1,59E-06	7,16E-07	4,56E-07	0,2231
C20:3	1,31E-06	8,78E-07	1,02E-06	3,31E-07	3,55E-07	1,66E-07	0,2789
AA C20:4	2,60E-05	1,47E-05	2,25E-05	1,18E-05	1,47E-06	9,51E-07	0,5065
AdA C22:4	1,90E-06	1,07E-06	1,42E-06	9,62E-07	2,86E-07	-	0,2540

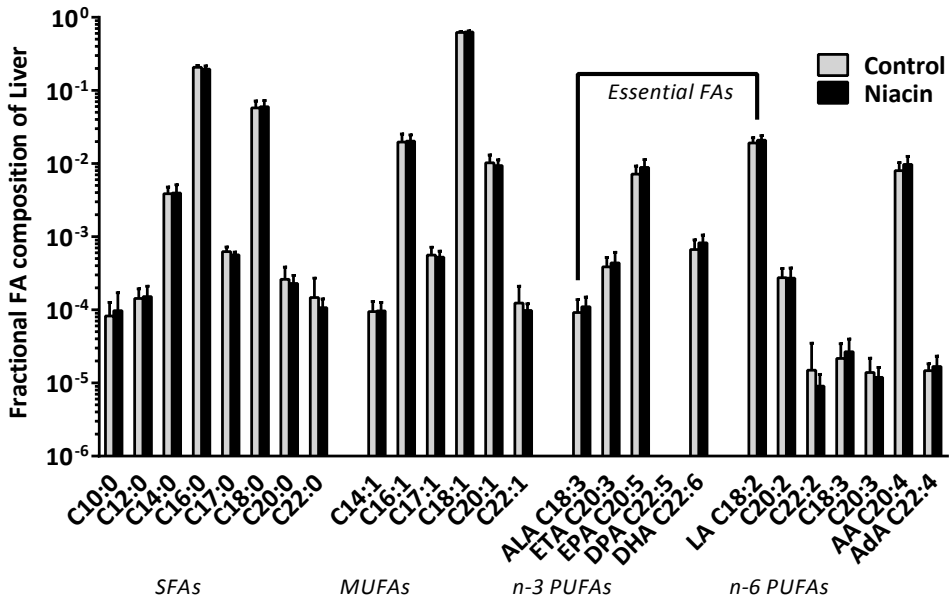

*Figure S2: Liver fatty acid composition from APOE*3-Leiden.CETP mice fed a western type diet with 0.1% cholesterol with and without niacin. Fraction of total area corrected sum. Mean±SD, N=14 for Control/N=13 for Niacin. *p<0.05 comparing control gWAT to niacin gWAT after false discovery rate correction.*

*Table S3: Liver fatty acid composition from APOE*3-Leiden.CETP mice fed a western type diet with 0.1% cholesterol with and without niacin. Fraction of total area corrected sum. Mean±SD, N=14 for Control/N=13 for Niacin. (*) Significant finding after false discovery rate correction.*

	Control Liver		Niacin Liver		Control vs Niacin
	Average	SD	Average	SD	P-value
SFA					
C10:0	8,23E-05	4,42E-05	9,74E-05	7,38E-05	0,5248
C12:0	0,000143	5,17E-05	0,000152	5,92E-05	0,6948
C14:0	0,003877	0,000907	0,003968	0,001167	0,8245
C16:0	0,20753	0,013181	0,196168	0,020302	0,0989
C17:0	0,000625	9,85E-05	0,000565	5,39E-05	0,0739
C18:0	0,057714	0,014338	0,059939	0,013182	0,6860
C20:0	0,000262	0,000122	0,000229	6,67E-05	0,4218
C22:0	0,000147	0,000125	0,000107	3,45E-05	0,2909
MUFA					
C14:1	9,46E-05	3,57E-05	9,7E-05	2,96E-05	0,8528
C16:1	0,019737	0,00563	0,020314	0,004366	0,7759
C17:1	0,00056	0,000161	0,000524	0,000112	0,5268
C18:1	0,621529	0,018559	0,628717	0,023243	0,3893
C20:1	0,010283	0,002869	0,009425	0,001852	0,3834
C22:1	0,000124	8,64E-05	9,79E-05	2,31E-05	0,3213
PUFA n-3					
ALA C18:3	9,17E-05	4,6E-05	0,00011	3,92E-05	0,2796
ETA C20:3	0,000388	0,000133	0,000438	0,000173	0,4111
EPA C20:5	0,00721	0,00204	0,00886	0,002503	0,0763
DPA C22:5	-	-	-	-	
DHA C22:6	0,000669	0,000237	0,000828	0,000228	0,0945
PUFA n-6					
LA C18:2	0,019119	0,003479	0,020887	0,003278	0,1973
C20:2	0,000276	9,29E-05	0,000271	0,000102	0,9115
C22:2	1,49E-05	2,02E-05	9,08E-06	4,02E-06	0,3334
C18:3	2,17E-05	1,29E-05	2,69E-05	1,31E-05	0,3204
C20:3	1,39E-05	7,87E-06	1,19E-05	4,41E-06	0,4437
AA C20:4	0,008023	0,002318	0,009784	0,002791	0,0916
AdA C22:4	1,47E-05	3,65E-06	1,69E-05	6,41E-06	0,3014

*Table S 4: Unfasted plasma PUFA and oxylipin concentrations of APOE*3-Leiden.CETP mice fed a western type diet with 0.1% cholesterol with and without niacin. Mean±SD, N=14 for Control/N=13 for Niacin. (*)Significant finding after false discovery rate correction.*

	Control		Niacin		Control vs Niacin
	Average (ng/mL)	**SD** (ng/mL)	**Average** (ng/mL)	**SD** (ng/mL)	**P-value**
PUFA					
ALA	1139,98	69,76	784,61	61,24	(*)0,0007
EPA	91,51	7,10	82,03	6,51	0,3342
DPA	1373,47	118,48	1133,20	81,11	0,0996
DHA	1012,96	52,65	1194,23	52,00	0,0226
LA	9033,60	427,04	8875,20	273,66	0,7614
AA	5833,59	417,18	5342,29	192,80	0,2949
AdA	139,25	11,33	119,86	7,21	0,1608
Oxylipins					
12-HETE	140,60	100,95	138,77	121,74	0,9666
Leukotriene E_4	0,125	0,020	0,112	0,005	0,0324
Prostaglandin D_2	0,545	0,073	0,528	0,097	0,6066
Thromboxane B_2	3,25	0,95	4,67	2,00	0,0252
14,15-diHETE	0,247	0,075	0,291	0,127	0,2891
19,20-diHDPA	0,696	0,131	1,011	0,345	(*)0,0065

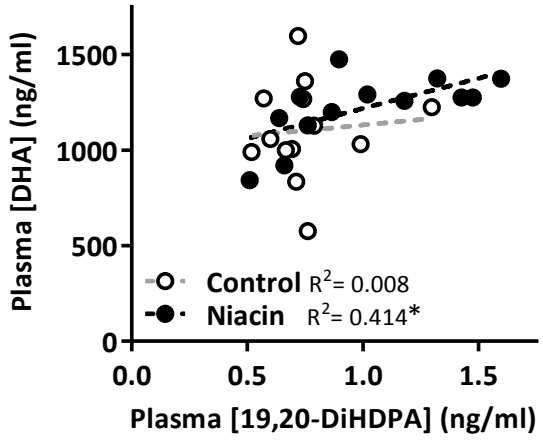

*Figure S3: Correlation between the plasma concentrations of 19,20-dihydroxydocosapentaenoic acid and docosahexaenoic acid. N=14 mice per group, *p<0.05 compared to a slope of zero.*

Table S5: Multiple Reaction Monitoring setup for ion transitions of the target compounds. Symbols in bold refer to internal standards. RT retention time, Q1 quadrupole 1 ion selection, Q3 quadrupole 3 ion selection, EP entrance potential, CE, collision energy, CCEP collision cell exit potential. HODEs, HOTrEs, HETEs, HEPEs, diHETEs and diHDPAs are given without chiral descriptors. Internal standards are indicated in grey.

Symbol	Lipid Maps ID	RT (min)	Q1 (m/z)	Q3 (m/z)	DP (Volts)	EP (Volts)	CE (Volts)	CCEP (Volts)
RvE1	LMFA03070019	4.0	349.1	195.0	-95	-10	-22	-13
20-hydroxy LTB_4	LMFA03020018	4.4	351.1	195.0	-60	-10	-24	-17
8-iso-$PGF_{2\alpha}$	LMFA03110001	5.1	353.1	193.0	-135	-10	-34	-11
15-keto-PGE_2	LMFA03010030	5.1	349.0	234.9	-65	-10	-20	-13
TxB_2	LMFA03030002	5.2	369.1	169.0	-55	-10	-24	-15
8-iso-PGE_2	LMFA03110003	5.3	351.1	271.0	-5	-10	-24	-19
13,14-dihydro-15-keto-PGE_2	LMFA03010031	5.6	351.1	235.0	-45	-10	-30	-13
PGE_2-d_4	LMFA03010008	5.6	355.1	193.0	-50	-10	-26	-17
PGE_2	LMFA03010003	5.7	351.2	271.1	-50	-10	-22	-21
PGD_2	LMFA03010004	5.8	351.1	233.0	-30	-10	-16	-13
LXB_4	LMFA03040002	6.0	351.1	220.9	-60	-10	-22	-13
$PGF_{2\alpha}$	LMFA03010002	6.1	353.1	193.0	-80	-10	-34	-11
RvD2	LMFA04000007	6.2	375.1	277.1	-60	-10	-18	-15
LXA_4	LMFA03040001	6.5	351.1	114.8	-40	-10	-20	-11
13,14-dihydro-15-keto-$PGF_{2\alpha}$	LMFA03010027	6.6	353.1	195.0	-110	-10	-32	-11
AT-RvD1	LMFA04000074	6.7	375.0	215.0	-50	-10	-26	-11
RvD1	LMFA04000006	6.7	375.1	215.0	-50	-10	-26	-11
epi-LXA_4	LMFA03040003	6.8	351.1	114.9	-20	-10	-22	-11
RvE2	LMFA03070036	7.8	333.1	114.9	-35	-10	-18	-15
18S-RvE3	LMFA03070048	8.8	333.1	245.2	-25	-10	-16	-17
6-trans-LTB_4	LMFA03020013	8.9	335.1	194.9	-105	-10	-22	-11
8S,15S-diHETE	LMFA03060050	8.9	335.1	207.9	-55	-10	-22	-17
LTD_4	LMFA03020006	9.0	495.1	177.0	-70	-10	-28	-19
6-trans-12-epi-LTB_4	LMFA03020014	9.1	335.1	194.9	-80	-10	-22	-25
10S,17S-diHDHA (PDX)	LMFA04000047	9.2	359.1	153.0	-70	-10	-22	-9
18R-RvE_3	LMFA03070049	9.2	333.1	245.0	-55	-10	-18	-23
7S-MaR1	n.a.	9.3	359.1	249.9	-20	-10	-20	-19
MaR1	LMFA04000048	9.4	359.2	250.2	-65	-10	-20	-13
LTB_4-d_4	LMFA03020030	9.4	339.1	196.9	-70	-10	-22	-19
LTB_4	LMFA03020001	9.4	335.1	195.0	-65	-10	-22	-21
14,15-diHETE	LMFA03060077	9.5	335.1	207.0	-65	-10	-24	-21
7,17-diHDPA	n.a.	9.5	361.1	198.9	-45	-10	-26	-23
LTE_4	LMFA03020002	9.6	438.1	333.1	-55	-10	-26	-15
19,20-diHDPA	LMFA04000043	10.2	361.1	273.0	-55	-10	-22	-15

Symbol	Lipid Maps ID	RT (min)	Q1 (m/z)	Q3 (m/z)	DP (Volts)	EP (Volts)	CE (Volts)	CCEP (Volts)
9-HOTrE	LMFA02000024	10.2	293.0	170.9	-75	-10	-20	-15
13-HOTrE	LMFA02000051	10.3	293.0	195.0	-45	-10	-24	-19
18-HEPE	LMFA03070038	10.4	317.1	259.0	-5	-10	-16	-7
15-HEPE	LMFA03070009	10.5	317.1	219.0	-65	-10	-18	-19
13-HODE	LMFA02000228	10.8	295.0	194.9	-110	-10	-24	-21
9-HODE	LMFA02000188	10.8	295.0	171.0	-130	-10	-22	-7
15-HETE-d_8	LMFA03060080	10.9	327.2	226.0	-85	-10	-18	-11
15-HETE	LMFA03060001	11.0	319.1	219.1	-55	-10	-18	-9
11-HETE	LMFA03060003	11.1	319.1	167.0	-70	-10	-22	-15
17-HDHA	LMFA04000072	11.1	343.1	245.0	-65	-10	-16	-15
12-HETE	LMFA03060007	11.2	319.1	179.0	-65	-10	-20	-23
8-HETE	LMFA03060006	11.2	319.1	154.9	-70	-10	-20	-19
5-HETE	LMFA03060002	11.3	319.1	115.0	-65	-10	-18	-11
ALA	LMFA01030152	12.4	277.0	233.0	-90	-10	-22	-29
EPA	LMFA01030759	12.4	301.0	202.9	-125	-10	-18	-21
DHA-d_5	LMFA01030762	12.4	332.0	288.1	-75	-10	-16	-13
DHA	LMFA01030185	12.7	327.1	229.2	-115	-10	-18	-11
AA	LMFA01030001	12.7	303.0	205.1	-155	-10	-20	-11
LA	LMFA01030120	12.8	279.0	261.0	-115	-10	-28	-13
DPA n-3	LMFA04000044	13.0	329.1	231.1	-50	-10	-20	-17
AdA	LMFA01030178	13.1	331.1	233.0	-130	-10	-22	-11

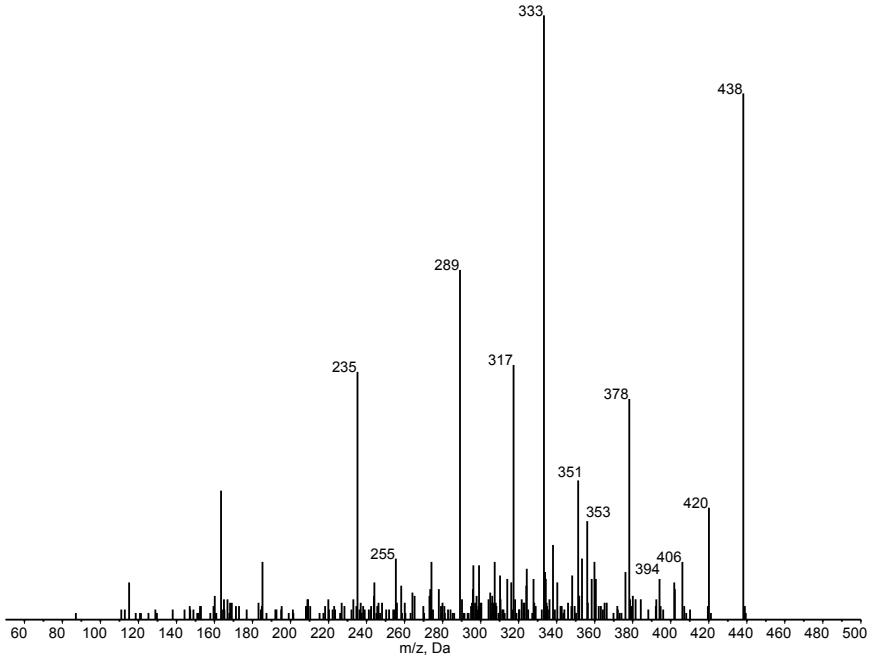

Figure S4a: MS/MS of 0.1 ng/mL standard sample at Relative RT 1.016 (Leukotriene E_4).

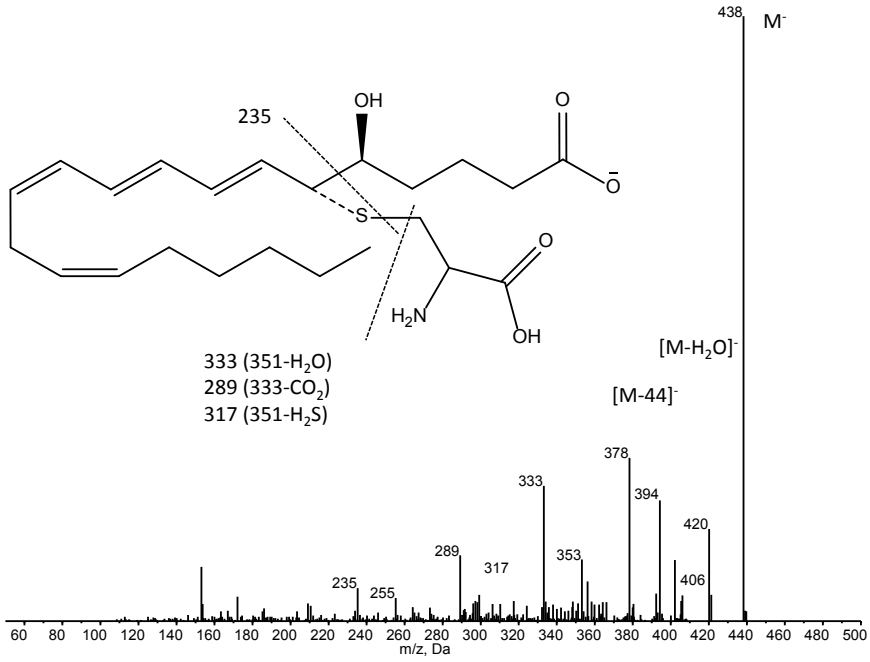

Figure S4b: MS/MS spectra of representative sample at Relative RT 1.015 (Leukotriene E_4).

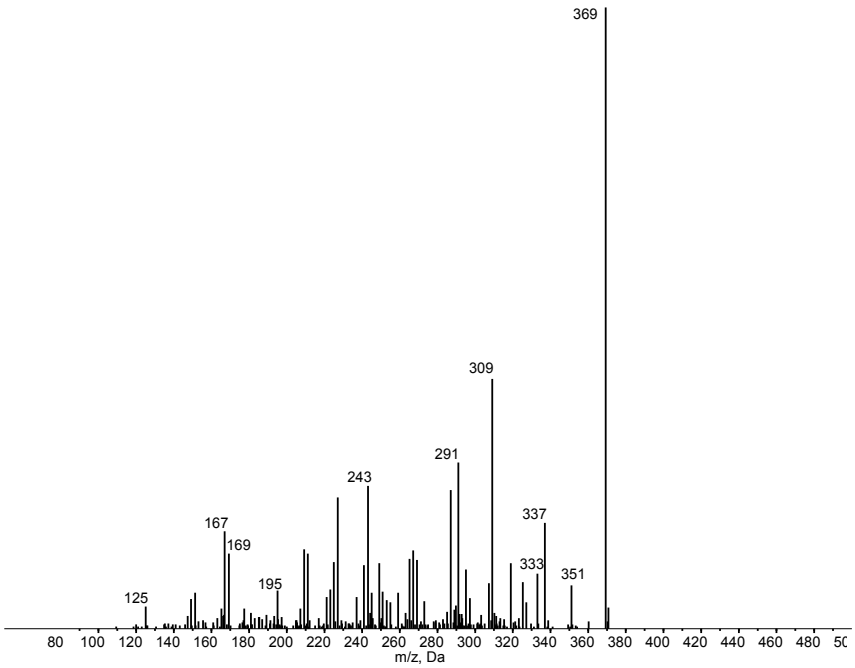

Figure S5a: MS/MS spectra of 0.1 ng/mL standard sample at Relative RT 0.925 (Thromboxane B_2).

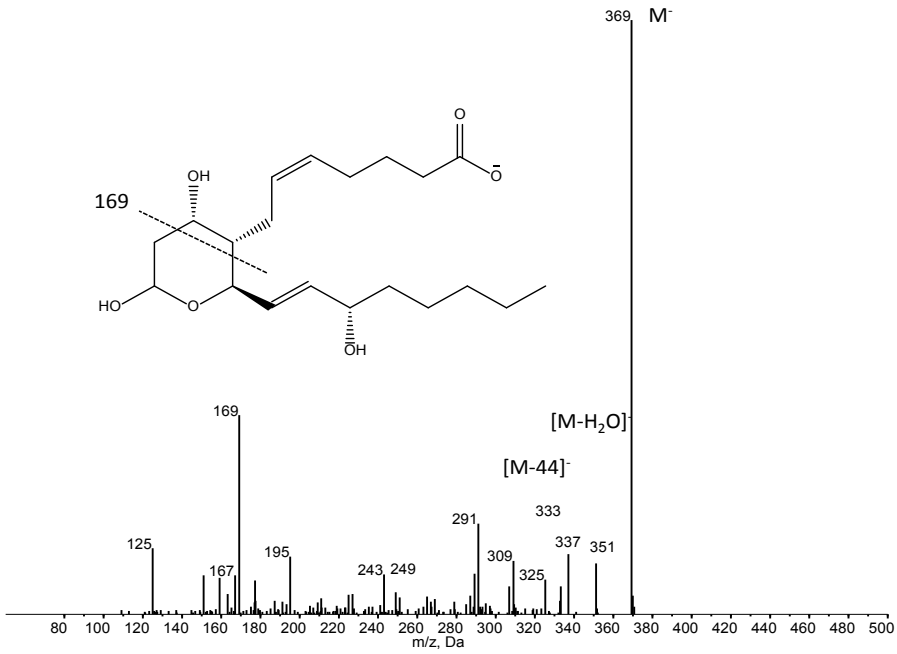

Figure S5b: MS/MS spectra of representative sample at Relative RT 0.927 (Thromboxane B_2).

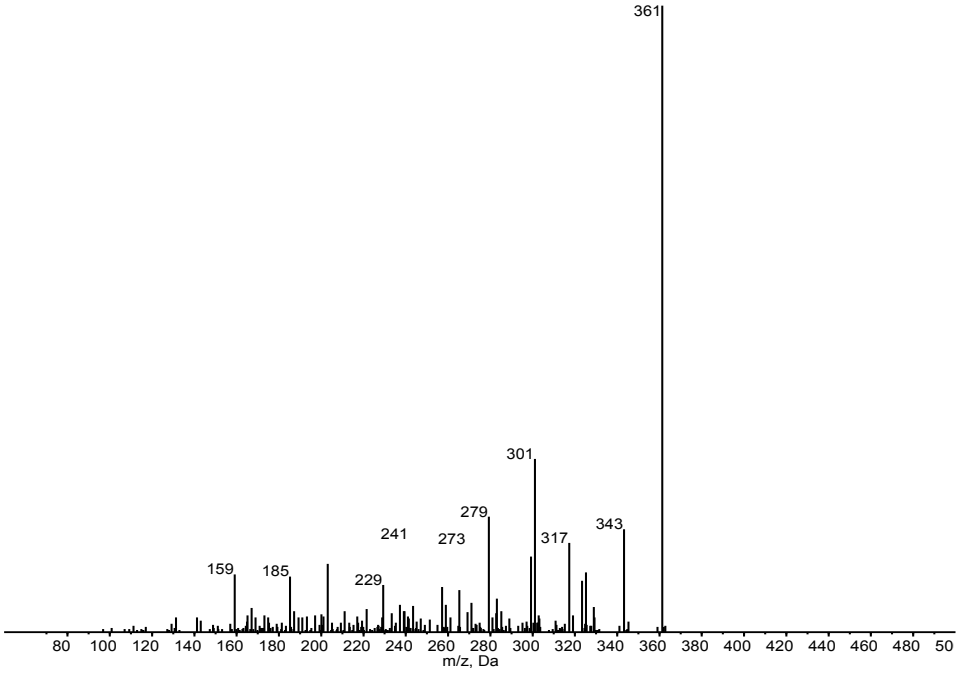

Figure S6a: MS/MS spectra of 0.1 ng/mL standard sample at Relative RT 1.087 (19,20-diHDPA).

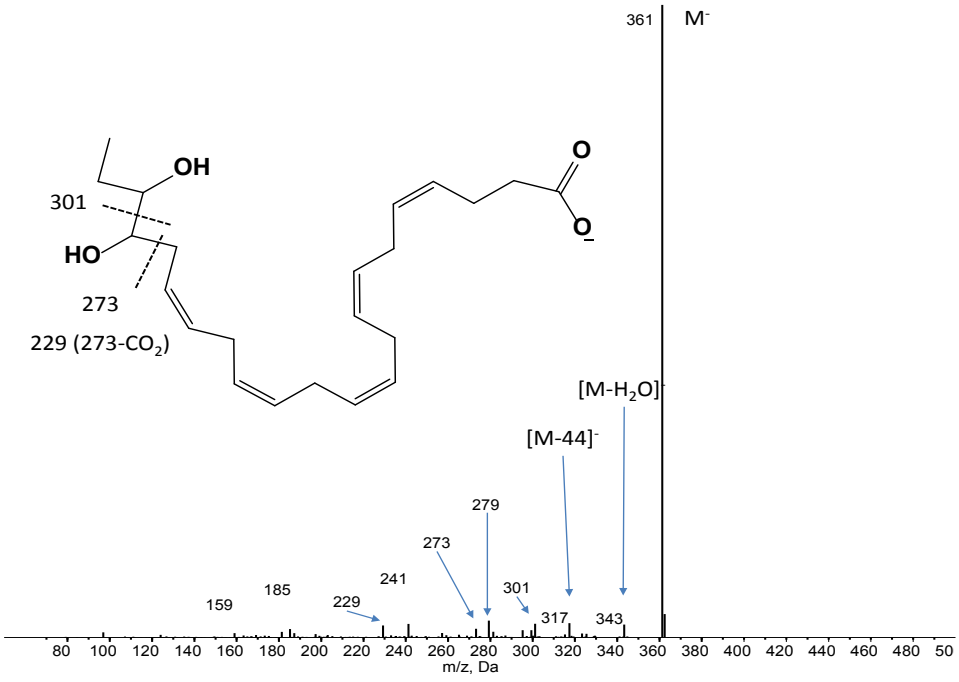

Figure S6b: MS/MS spectra of representative sample at Relative RT 1.087 (19,20-diHDPA).

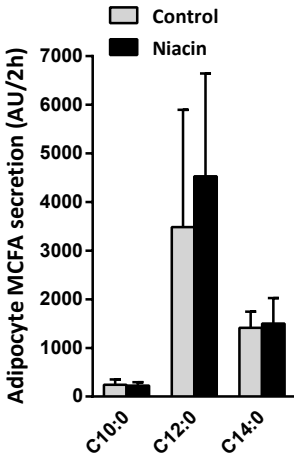

*Figure S7: Release of medium chain saturated fatty acids from adipocytes isolated from APOE*3-Leiden.CETP mice fed a western type diet with 0.1% cholesterol with and without niacin. Fatty acid release in arbitrary units during a 2 hour ex vivo basal incubation. Mean±SD, N=14 for Control/N=13 for Niacin.*

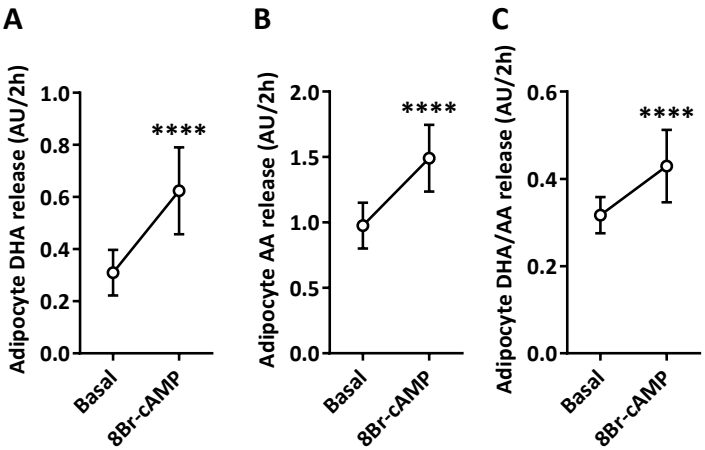

*Figure S8: Release of DHA and AA from adipocytes isolated from APOE*3-Leiden.CETP mice fed a western type diet with 0.1% cholesterol without niacin. Fatty acid release in arbitrary units during a 2 hour ex vivo incubation in basal and 8Bromo-cAMP stimulated conditions. Mean±SD, N=14 for Control/N=13 for Niacin. **** p<0,0001 for Basal vs 8Br-cAMP.*

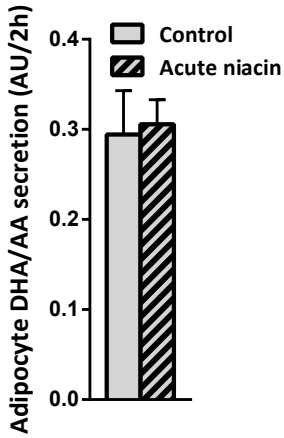

*Figure S9: Ratio of DHA/AA released fatty acids from adipocytes isolated from APOE*3-Leiden.CETP mice fed a western type diet with 0.1% cholesterol without niacin. Fatty acid release in arbitrary units during a 2 hour ex vivo incubation under basal and acute niacin conditions. Mean±SD, N=14 for Control/N=10 for Acute niacin.*